

Isometric Energies for Recovering Injectivity in Constrained Mapping

(Supplemental Materials)

This document completes the derivations and proofs absent from the main paper (Sections 1-4), and provides additional implementation details (Section 5) and experimental results (Section 6).

1 Singular value formula for lifted content

We will derive the alternative formula of lifted content (Equation 4 in the paper). Given two d -dimensional simplices t, \tilde{t} (\tilde{t} has positive d -dimensional volume) and scalar $\alpha > 0$, the *lifted content* of t is defined as:

$$A_{\tilde{t},\alpha}(t) = \frac{1}{d!} \sqrt{\det(X^T X + \alpha \tilde{X}^T \tilde{X})} \quad (1)$$

where X, \tilde{X} are the edge (column) vectors of t, \tilde{t} respectively.

Let L be the linear transformation that maps \tilde{t} to t , that is, $L = X \tilde{X}^{-1}$ (note that \tilde{X} is always invertible because \tilde{t} has positive content). Applying Sylvester's Theorem to the determinant inside the square root yields:

$$\begin{aligned} \det(X^T X + \alpha \tilde{X}^T \tilde{X}) &= \det(\alpha \tilde{X}^T \tilde{X}) \det(I_d + \frac{1}{\alpha} X \tilde{X}^{-1} (\tilde{X}^T)^{-1} X^T) \\ &= \det(\tilde{X}^T \tilde{X}) \det(\alpha I_d + X \tilde{X}^{-1} (\tilde{X}^{-1})^T X^T) \\ &= \det(\tilde{X}^T \tilde{X}) \det(\alpha I_d + LL^T) \end{aligned} \quad (2)$$

where I_d is the $d \times d$ identity matrix. Consider the singular value decomposition $L = U \Sigma V^T$, where U, V are orthonormal matrices and Σ is a diagonal matrix whose diagonal entries are the singular values $\{\sigma_1, \dots, \sigma_d\}$. We can simplify the last determinant in Equation 2 as:

$$\begin{aligned} \det(\alpha I_d + LL^T) &= \det(\alpha I_d + U \Sigma V^T V \Sigma^T U^T) \\ &= \det(U(\alpha I_d) U^T + U \Sigma \Sigma^T U^T) \\ &= \det(U(\alpha I_d + \Sigma \Sigma^T) U^T) \\ &= \det(U) \det(\alpha I_d + \Sigma \Sigma^T) \det(U^T) \\ &= \det(\alpha I_d + \Sigma \Sigma^T) \\ &= \prod_{i=1}^d (\sigma_i^2 + \alpha) \end{aligned} \quad (3)$$

The last equality holds because $\alpha I_d + \Sigma \Sigma^T$ is a diagonal matrix whose diagonal values are $\{\sigma_1^2 + \alpha, \dots, \sigma_d^2 + \alpha\}$. Substituting Equation 3 into Equation 2 and then into Equation 1 yields:

$$\begin{aligned} A_{\tilde{t},\alpha}(t) &= \frac{1}{d!} \sqrt{\det(\tilde{X}^T \tilde{X}) \prod_{i=1}^d (\sigma_i^2 + \alpha)} \\ &= A_{\tilde{t}} \sqrt{\prod_{i=1}^d (\sigma_i^2 + \alpha)} \end{aligned} \quad (4)$$

where $A_{\tilde{t}}$ is the volume of \tilde{t} .

2 Minimizer of residue functions

We will prove Propositions 2.1 and 2.2 in the paper regarding the minimizer of functions $R(t)$ and $R^{iso}(t)$. Recall that $R(t)$ is the residue of the lifted content $A_{\tilde{t},\alpha}(t)$ of a simplex t after subtracting the signed volume $A(t)$, and it has the form (Equation 5 in the paper):

$$R(t) = A_{\tilde{t}}(\sqrt{\prod_{i=1}^d (\sigma_i^2 + \alpha)} - \det(L)). \quad (5)$$

Similarly, $R^{iso}(t)$ is the residue of the isometric lifted content $A_{\tilde{t},\alpha}^{iso}(t)$ after subtracting $A(t)$, and it has the form (Equation 8 in the paper):

$$R^{iso}(t) = A_{\tilde{t}}(\sqrt{\prod_{i=1}^d \sigma_i^2 + \frac{\alpha}{2^{d-1}} \prod_{i=1}^d (\sigma_i^2 + 1) + \alpha^2} - \det(L)). \quad (6)$$

We first prove that $R(t)$ is minimized by similarity transformations in 2D and a singular transformation in higher dimensions:

Proposition 2.1 (Proposition 2.1 in paper). *For any $\alpha > 0$, $R(t) \geq \alpha^{\frac{d}{2}} A_{\tilde{t}}$. Equality holds when either of the following holds:*

1. $d = 2$, $\sigma_1 = \sigma_2$ and $\det(L) \geq 0$.
2. $d > 2$ and $\sigma_1 = \dots = \sigma_d = 0$.

Proof. Using the definition of $R(t)$ in Equation 5, and since $A_{\tilde{t}} > 0$, we only need to show that

$$\sqrt{\prod_{i=1}^d (\sigma_i^2 + \alpha)} \geq \det(L) + \alpha^{\frac{d}{2}} \quad (7)$$

We first consider the case of $d = 2$. The lhs of Equation 7 becomes:

$$\begin{aligned} \sqrt{(\sigma_1^2 + \alpha)(\sigma_2^2 + \alpha)} &= \sqrt{(\sigma_1 \sigma_2 + \alpha)^2 + \alpha(\sigma_1^2 + \sigma_2^2 - 2\sigma_1 \sigma_2)} \\ &\geq \sqrt{(\sigma_1 \sigma_2 + \alpha)^2} \\ &= \sigma_1 \sigma_2 + \alpha \\ &= |\det(L)| + \alpha \\ &\geq \det(L) + \alpha \end{aligned}$$

The first inequality becomes equality when $\sigma_1 = \sigma_2$, and the second inequality becomes equality when $\det(L) \geq 0$.

Now consider $d \geq 3$, which we split into two cases.

1. Suppose $\prod_{i=1}^d \sigma_i = 0$ (and hence $\det(L) = 0$). It follows that:

$$\sqrt{\prod_{i=1}^d (\sigma_i^2 + \alpha)} \geq \sqrt{\alpha^d} = \det(L) + \alpha^{\frac{d}{2}}$$

The inequality becomes equality only when $\sigma_1 = \dots = \sigma_d = 0$.

2. Now suppose $\prod_{i=1}^d \sigma_i > 0$. We can derive from the lhs of Equation 7 that:

$$\begin{aligned}
\sqrt{\prod_{i=1}^d (\sigma_i^2 + \alpha)} &\geq \sqrt{(\prod_{i=1}^d \sigma_i)^2 + \alpha^d + \alpha^{d-1} \sum_{i=1}^d \sigma_i^2 + \alpha \sum_{i=1}^d \frac{\prod_{j=1}^d \sigma_j^2}{\sigma_i^2}} \\
&= \sqrt{(\prod_{i=1}^d \sigma_i + \alpha^{\frac{d}{2}})^2 - 2\alpha^{\frac{d}{2}} \prod_{i=1}^d \sigma_i + \alpha^{\frac{d}{2}} (\prod_{i=1}^d \sigma_i) \sum_{i=1}^d \left(\frac{\alpha^{\frac{d}{2}-1} \sigma_i^2}{\prod_{j=1}^d \sigma_j} + \frac{\prod_{j=1}^d \sigma_j}{\alpha^{\frac{d}{2}-1} \sigma_i^2} \right)} \\
&= \sqrt{(\prod_{i=1}^d \sigma_i + \alpha^{\frac{d}{2}})^2 + \alpha^{\frac{d}{2}} (\prod_{i=1}^d \sigma_i) \left(\sum_{i=1}^d \left(\frac{\alpha^{\frac{d}{2}-1} \sigma_i^2}{\prod_{j=1}^d \sigma_j} + \frac{\prod_{j=1}^d \sigma_j}{\alpha^{\frac{d}{2}-1} \sigma_i^2} \right) - 2 \right)} \\
&\geq \sqrt{(\prod_{i=1}^d \sigma_i + \alpha^{\frac{d}{2}})^2 + \alpha^{\frac{d}{2}} (\prod_{i=1}^d \sigma_i) (2d - 2)} \\
&> \sqrt{(\prod_{i=1}^d \sigma_i + \alpha^{\frac{d}{2}})^2} \\
&= |\det(L)| + \alpha^{\frac{d}{2}} \\
&\geq \det(L) + \alpha^{\frac{d}{2}}
\end{aligned}$$

The second inequality is due to the fact that $x + \frac{1}{x} \geq 2$ for any positive x .

Combining the two cases, we have proved Equation 7 for $d \geq 3$. In particular, the equality holds only in the first case, that is, when $\sigma_1 = \dots = \sigma_d = 0$. \square

We next prove that $R^{iso}(t)$ is minimized by an isometry in any dimensions:

Proposition 2.2 (Proposition 2.2 in paper). *For any $\alpha > 0$, $R^{iso}(t) \geq \alpha A_{\tilde{t}}$, and equality holds only when $\sigma_1 = \dots = \sigma_d = 1$ and $\det(L) > 0$.*

Proof. Using the definition of $R^{iso}(t)$ in Equation 6, and since $A_{\tilde{t}} > 0$, we need to show that

$$\sqrt{\prod_{i=1}^d \sigma_i^2 + \frac{\alpha}{2^{d-1}} \prod_{i=1}^d (\sigma_i^2 + 1) + \alpha^2} \geq \det(L) + \alpha \quad (8)$$

We consider two cases for any $d \geq 2$:

1. Suppose $\prod_{i=1}^d \sigma_i = 0$ (and hence $\det(L) = 0$). The lhs of Equation 8 becomes:

$$\sqrt{\frac{\alpha}{2^{d-1}} \prod_{i=1}^d (\sigma_i^2 + 1) + \alpha^2} > \alpha = \det(L) + \alpha$$

Note that the inequality is strict, because the first term under the square root is always positive.

2. Now suppose $\prod_{i=1}^d \sigma_i > 0$. We have the following derivation from the lhs of Equation 8:

$$\begin{aligned}
\sqrt{\prod_{i=1}^d \sigma_i^2 + \frac{\alpha}{2^{d-1}} \prod_{i=1}^d (\sigma_i^2 + 1) + \alpha^2} &= \sqrt{(\prod_{i=1}^d \sigma_i + \alpha)^2 - 2\alpha \prod_{i=1}^d \sigma_i + \frac{\alpha}{2^{d-1}} \prod_{i=1}^d (\sigma_i^2 + 1)} \\
&= \sqrt{(\prod_{i=1}^d \sigma_i + \alpha)^2 + 2\alpha (\prod_{i=1}^d \sigma_i) \left(\frac{1}{2^d} \prod_{i=1}^d (\sigma_i + \frac{1}{\sigma_i}) - 1 \right)} \\
&\geq \sqrt{(\prod_{i=1}^d \sigma_i + \alpha)^2} \\
&= \prod_{i=1}^d \sigma_i + \alpha \\
&= |\det(L)| + \alpha \\
&\geq \det(L) + \alpha
\end{aligned}$$

The second inequality is again due to the fact that $x + \frac{1}{x} \geq 2$ for any positive x , and it becomes equality when $\sigma_1 = \dots = \sigma_d = 1$, which turns the last inequality into equality as well.

We conclude from both cases that Equation 8 holds for all $d \geq 2$, and it becomes equality only when $\sigma_1 = \dots = \sigma_d = 1$. \square

3 Injectivity of IsoTLC minimizer

We will prove Proposition 2.3 in the paper on the injectivity of the energy minimizer of IsoTLC. Recall that the *isometric lifted content* of a simplex t , given the auxiliary simplex \tilde{t} and scalar α , has the following form (Equation 6 in the paper),

$$A_{\tilde{t},\alpha}^{iso}(t) = \sqrt{A(t)^2 + \frac{\alpha}{2^{d-1}} A_{\tilde{t},1}(t)^2 + \alpha^2 A_{\tilde{t}}^2}, \quad (9)$$

where $A_{\tilde{t},1}(t)$ is the lifted content of t at scale 1. The *Isometric Total Lifted Content* (IsoTLC) for a mesh T , given auxiliary elements \tilde{T} and scalar α , is the sum,

$$A_{\tilde{T},\alpha}^{iso}(T) = \sum_{t \in T} A_{\tilde{t},\alpha}^{iso}(t). \quad (10)$$

We start with a lemma:

Lemma 3.1. *The following holds for all $\alpha \geq 0$:*

1. $A_{\tilde{t},\alpha}^{iso}(t) \geq |A(t)|$, and equality holds when $\alpha = 0$.
2. The derivative $\frac{\partial A_{\tilde{t},\alpha}^{iso}(t)}{\partial \alpha}$ is finite and positive if either $A(t) \neq 0$ or $\alpha \neq 0$.

Proof. Statement (1) is straightforward from Equation 9 by noting that the second and third terms under the square root are non-negative and zero only when $\alpha = 0$. For (2), substituting Equation 9 into the derivative gives:

$$\frac{\partial A_{\tilde{t},\alpha}^{iso}(t)}{\partial \alpha} = \frac{\frac{A_{\tilde{t},1}(t)^2}{2^{d-1}} + 2\alpha A_{\tilde{t}}^2}{2\sqrt{A(t)^2 + \frac{\alpha}{2^{d-1}} A_{\tilde{t},1}(t)^2 + \alpha^2 A_{\tilde{t}}^2}} \quad (11)$$

Assuming that either $A(t) \neq 0$ or $\alpha \neq 0$, the denominator of the rhs is non-zero, and hence the derivative is well-defined. Also, since the lifted content $A_{\tilde{t},1}(t)$ is always positive, the numerator is strictly positive, and so is the derivative. \square

We next prove a lemma that plays the same role as Lemma B.3 (2D) or B.7 (3D) in [1] in their proof of the injectivity of TLC minimizer. Unlike TLC, where the statement requires different proofs in 2D and 3D and the validity of the statement is unknown in higher dimensions, our statement on IsoTLC applies to any dimension $d \geq 2$.

Lemma 3.2. *For any $\delta > 0$, there exists some $\epsilon > 0$ and $\beta > 0$ such that if a map T contains an element whose unsigned volume is smaller than ϵ , then for any positive $\alpha < \beta$, $\partial A_{\tilde{T},\alpha}^{iso}(T)/\partial \alpha > \delta$.*

Proof. Consider a single element $t \in T$. Using the lifted content formula of Equation 4, we have

$$A_{\tilde{t},1}(t) = A_{\tilde{t}} \sqrt{\prod_{i=1}^d (\sigma_i^2 + 1)} \geq A_{\tilde{t}}$$

Using this inequality, we can derive from the derivative formula of Equation 11 for any $\alpha > 0$:

$$\begin{aligned} \frac{\partial A_{\tilde{t},\alpha}^{iso}(t)}{\partial \alpha} &> \frac{A_{\tilde{t},1}(t)^2}{2^d \sqrt{A(t)^2 + \frac{\alpha}{2^{d-1}} A_{\tilde{t},1}(t)^2 + \alpha^2 A_{\tilde{t}}^2}} \\ &= \frac{1}{2^d \sqrt{\frac{A(t)^2}{A_{\tilde{t},1}(t)^4} + \frac{\alpha}{2^{d-1}} \frac{A_{\tilde{t},1}(t)^2}{A_{\tilde{t},1}(t)^4} + \frac{\alpha^2 A_{\tilde{t}}^2}{A_{\tilde{t},1}(t)^4}}} \\ &\geq \frac{1}{2^d \sqrt{\frac{A(t)^2}{A_{\tilde{t}}^4} + \frac{\alpha}{2^{d-1}} \frac{A_{\tilde{t}}^2}{A_{\tilde{t}}^4} + \frac{\alpha^2 A_{\tilde{t}}^2}{A_{\tilde{t}}^4}}} \\ &= \frac{A_{\tilde{t}}^2}{2^d \sqrt{A(t)^2 + A_{\tilde{t}}^2 \left(\frac{\alpha}{2^{d-1}} + \alpha^2 \right)}} \end{aligned}$$

For any $\delta > 0$, we can find $\epsilon > 0, \beta > 0$ that satisfies:

$$\epsilon^2 + A_t^2 \left(\frac{\beta}{2^{d-1}} + \beta^2 \right) = \frac{A_t^4}{2^{2d} \delta^2}$$

If $|A(t)| < \epsilon$ and $\alpha \in (0, \beta)$, we conclude that:

$$\frac{\partial A_{t,\alpha}^{iso}(t)}{\partial \alpha} > \frac{A_t^2}{2^d \sqrt{A(t)^2 + A_t^2 \left(\frac{\alpha}{2^{d-1}} + \alpha^2 \right)}} > \frac{A_t^2}{2^d \sqrt{\epsilon^2 + A_t^2 \left(\frac{\beta}{2^{d-1}} + \beta^2 \right)}} = \delta$$

Finally, let t_0 be an element of T such that $|A(t_0)| < \epsilon$. Combining the inequality above and Lemma 3.1 (2) yields the desired inequality for all $\alpha \in (0, \beta)$,

$$\frac{\partial A_{\tilde{T},\alpha}^{iso}(T)}{\partial \alpha} = \sum_{t \in T} \frac{\partial A_{t,\alpha}^{iso}(t)}{\partial \alpha} > \frac{\partial A_{t_0,\alpha}^{iso}(t_0)}{\partial \alpha} > \delta$$

□

Finally, we prove the main result for any $d \geq 2$:

Proposition 3.3 (Proposition 2.3 in the paper). *Let T_0 be an injective map with a fully constrained boundary and possible interior constraints. Then there exists some $\alpha_0 > 0$ such that $A_{\tilde{T},\alpha}^{iso}(T) > A_{\tilde{T},\alpha}^{iso}(T_0)$ for any $\alpha < \alpha_0$ and any non-injective map T satisfying the same constraints.*

Proof. The proof closely follows that of Proposition 4.3 in [1]. Since T_0 is injective, so is the boundary map ∂T_0 from ∂M . By [6], a map T whose boundary is the same as ∂T_0 is injective if and only if T has no degenerate or inverted elements. In the following, we assume that an arbitrary but fixed set of auxiliary elements \tilde{T} is used. For notational convenience, we shall drop the subscript \tilde{T} in $A_{\tilde{T},\alpha}^{iso}$.

By Lemma 3.1 (2), and since T_0 is injective, the derivative $\partial A_{\alpha}^{iso}(T_0)/\partial \alpha$ is bounded. We shall pick an arbitrary but small positive value τ , and define δ as the maximum derivative for all $\alpha < \tau$.

Now suppose T has an element whose unsigned volume is smaller than ϵ , which is found by Lemma 3.2 for δ . By that lemma, there exists some $\beta > 0$ such that for any $\alpha < \beta$, $\partial A_{\alpha}^{iso}(T)/\partial \alpha > \delta$. As a result, the following holds for all $\alpha < \min(\tau, \beta)$:

$$\frac{\partial (A_{\alpha}^{iso}(T) - A_{\alpha}^{iso}(T_0))}{\partial \alpha} = \frac{\partial A_{\alpha}^{iso}(T)}{\partial \alpha} - \frac{\partial A_{\alpha}^{iso}(T_0)}{\partial \alpha} > \delta - \delta = 0$$

Furthermore, by Lemma 3.1 (a), $A_0^{iso}(T)$ is the total unsigned volume of T , which is no smaller than the total unsigned volume of T_0 , or $A_0^{iso}(T_0)$. Thus we conclude $A_{\alpha}^{iso}(T) > A_{\alpha}^{iso}(T_0)$ for any $\alpha \in (0, \min(\tau, \beta))$.

Otherwise, suppose T has no element whose unsigned volume is smaller than ϵ . Since T is non-injective, it must contain no degenerate element and at least one inverted element whose unsigned volume is at least ϵ . Due to Lemma 3.1 (1), for any $\alpha > 0$,

$$A_{\alpha}^{iso}(T) > \sum_{t \in T} |A(t)| \geq \sum_{t \in T} A(t) + 2\epsilon = A_0^{iso}(T_0) + 2\epsilon$$

Since the derivative $\partial A_{\alpha}^{iso}(T_0)/\partial \alpha$ is bounded (Lemma 3.2), there exists some $\kappa > 0$ such that, for all $\alpha < \kappa$,

$$A_{\alpha}^{iso}(T_0) < A_0^{iso}(T_0) + 2\epsilon < A_{\alpha}^{iso}(T)$$

The proof is completed by letting $\alpha_0 = \min(\tau, \beta, \kappa)$. □

4 Injectivity of IsoSEA minimizer

Lastly, we will prove Proposition 2.4 in the paper on the injectivity of the energy minimizer of IsoSEA. Recall that the *Isometric Smooth Excess Area* (IsoSEA) of a triangular mesh T , given the auxiliary simplices \tilde{T} and scalars α, θ , has the following form (Equation 11 in the paper):

$$A_{\tilde{T}, \alpha, \theta}^{iso}(T) = A_{\tilde{T}, \alpha}^{iso}(T) - O_\theta(\partial T). \quad (12)$$

where $A_{\tilde{T}, \alpha}^{iso}(T)$ is the IsoTLC of T and $O_\theta(\partial T)$ is the *arc-occupancy* of the boundary ∂T defined as follows. Recall that the *occupancy* $O(C)$ of a closed curve C is the area of the plane with a positive winding number w.r.t. C . Let C_θ be a curve constructed by replacing each edge of ∂T by an arc with center angle θ . The arc-occupancy $O_\theta(\partial T)$ is defined as the occupancy of C_θ subtracted by the total area of the regions each bounded by an edge of ∂T and its arc in C_θ .

We first recall a few useful properties of the *excess area* of T defined as the difference:

$$A^{excess}(T) = \sum_{t \in T} |A(t)| - O(\partial T)$$

Furthermore, let $A^{overlap}(T)$ be the total overlapping area defined as the difference between the total unsigned area of triangles in T and the area of the plane covered by T , and let $A^{invert}(T)$ be the total area of inverted triangles in T . The following result from [2] shows that the excess area is a good proxy of both the overlapping and inverted area:

Lemma 4.1 (Proposition 5.1 in [2]). *For any map T ,*

1. $A^{excess}(T) \geq A^{overlap}(T)$
2. $A^{excess}(T) \geq A^{invert}(T)$
3. $A^{excess}(T) \leq A^{overlap}(T) + A^{invert}(T)$

Using these results, we prove a property of IsoSEA similar to that of SEA in Proposition 5.2 of [2]:

Lemma 4.2. *For any map T , $\alpha \geq 0$ and $\theta > 0$, $A_{\tilde{T}, \alpha, \theta}^{iso}(T) \geq A^{excess}(T)$. Furthermore, if T is injective, there exists some $\theta_0 > 0$ such that $A_{\tilde{T}, 0, \theta}^{iso}(T) = 0$ for all $\theta < \theta_0$.*

Proof. The proof of Proposition 5.2 in [2] utilizes Lemma 4.1 and the fact that TLC is an upper bound of the total unsigned area, that is, $A_{\tilde{T}, \alpha}(T) \geq \sum_{t \in T} |A(t)|$. Since the same property holds for IsoTLC (Lemma 3.1 (1)), the rest of the proof follows. \square

Next, we introduce a variant of Lemma 3.2 that concerns maps containing triangles with large angle distortions. Let $D_{\tilde{t}}(t)$ be the Dirichlet energy of the transformation from a triangle t back to its auxiliary triangle \tilde{t} , which has the form [7] (utilizing the fact that the singular values of this inverse transform are reciprocals of σ_1, σ_2 , the singular values of the transform from \tilde{t} to t):

$$D_{\tilde{t}}(t) = \frac{|A(t)|}{2} \left(\frac{1}{\sigma_1^2} + \frac{1}{\sigma_2^2} \right) = \frac{A_{\tilde{t}}}{2} \left(\frac{\sigma_1^2 + \sigma_2^2}{\sigma_1 \sigma_2} \right) \quad (13)$$

The second equality comes from $|A(t)| = A_{\tilde{t}} \sigma_1 \sigma_2$. Note that the energy is minimal when $\sigma_1 = \sigma_2$ (no angle distortion).

Lemma 4.3. *For any $\delta > 0$, there exists some $\eta > 0$ and $\gamma > 0$ such that if a map T has no degenerate triangle but contains a triangle t such that $D_{\tilde{t}}(t) > \eta$, then for any positive $\alpha < \gamma$, $\partial A_{\tilde{T}, \alpha}^{iso}(T)/\partial \alpha > \delta$.*

Proof. Consider a single element $t \in T$ ($A(t) \neq 0$ by assumption). We first derive the following inequality using equality $|A(t)| = A_{\tilde{t}} \sigma_1 \sigma_2$ and Equations 4 and 13,

$$\frac{A_{t,1}^2(t)}{|A(t)|} = \frac{A_{\tilde{t}}^2(\sigma_1^2 + 1)(\sigma_2^2 + 1)}{A_{\tilde{t}} \sigma_1 \sigma_2} > \frac{A_{\tilde{t}}(\sigma_1^2 + \sigma_2^2)}{\sigma_1 \sigma_2} = 2D_{\tilde{t}}(t).$$

Recall from the proof of Lemma 3.2 that, for any $\alpha > 0$:

$$\frac{\partial A_{\tilde{t},\alpha}^{iso}(t)}{\partial \alpha} > \frac{1}{2^d \sqrt{\frac{A(t)^2}{A_{\tilde{t},1}(t)^4} + \frac{\alpha}{2^{d-1}} \frac{\alpha}{A_{\tilde{t},1}(t)^2} + \frac{\alpha^2 A_{\tilde{t}}^2}{A_{\tilde{t},1}(t)^4}}}$$

Continuing the derivation using the inequalities $\frac{A_{\tilde{t},1}^2(t)}{|A(t)|} > 2D_{\tilde{t}}(t)$ and $A_{\tilde{t},1}(t) > A_{\tilde{t}}$ yields

$$\begin{aligned} \frac{\partial A_{\tilde{t},\alpha}^{iso}(t)}{\partial \alpha} &> \frac{1}{2^d \sqrt{\frac{1}{4D_{\tilde{t}}^2(t)} + \frac{\alpha}{2^{d-1}} \frac{\alpha}{A_{\tilde{t}}^2} + \frac{\alpha^2 A_{\tilde{t}}^2}{A_{\tilde{t}}^4}}} \\ &= \frac{A_{\tilde{t}}}{2^d \sqrt{\frac{A_{\tilde{t}}^2}{4D_{\tilde{t}}^2(t)} + \frac{\alpha}{2^{d-1}} + \alpha^2}} \end{aligned}$$

For any $\delta > 0$, we can find $\eta > 0, \gamma > 0$ that satisfies:

$$\frac{A_{\tilde{t}}^2}{4\eta^2} + \frac{\gamma}{2^{d-1}} + \gamma^2 = \frac{A_{\tilde{t}}^2}{2^{2d}\delta^2}$$

If $D_{\tilde{t}}(t) > \eta$ and $\alpha \in (0, \gamma)$, we conclude that:

$$\frac{\partial A_{\tilde{t},\alpha}^{iso}(t)}{\partial \alpha} > \frac{A_{\tilde{t}}}{2^d \sqrt{\frac{A_{\tilde{t}}^2}{4D_{\tilde{t}}^2(t)} + \frac{\alpha}{2^{d-1}} + \alpha^2}} > \frac{A_{\tilde{t}}}{2^d \sqrt{\frac{A_{\tilde{t}}^2}{4\eta^2} + \frac{\gamma}{2^{d-1}} + \gamma^2}} = \delta$$

Finally, let t_0 be an element of T such that $D_{\tilde{t}_0}(t_0) > \eta$. Combining the inequality above and Lemma 3.1 (2) yields the desired inequality for all $\alpha \in (0, \gamma)$,

$$\frac{\partial A_{\tilde{T},\alpha}^{iso}(T)}{\partial \alpha} = \sum_{t \in T} \frac{\partial A_{\tilde{t},\alpha}^{iso}(t)}{\partial \alpha} > \frac{\partial A_{t_0,\alpha}^{iso}(t_0)}{\partial \alpha} > \delta$$

□

We will also need the following result from [2]. It gives a lower bound of the overlapping area around an overwound vertex as a function of the minimum triangle area and maximum per-triangle Dirichlet energy.

Lemma 4.4 (Lemma D.4 in [2]). *If map T contains an interior vertex v such that v is incident to only triangles with positive areas and the sum of angles around v is not 2π , then $A^{overlap}(T) \geq \epsilon h^2 \pi / 2\eta$, where ϵ is the minimum unsigned area of any triangle in T , h is the shortest height of any auxiliary triangle in \tilde{T} , and η is the maximum $D_{\tilde{t}}(t)$ in any $t \in T$.*

We are ready to prove the main result:

Proposition 4.5 (Proposition 2.4 in the paper). *Let T_0 be an injective, triangular map satisfying the given constraints. For any $\lambda > 0$, there exists some $\alpha_0 > 0$ and $\theta_0 > 0$ such that, for any $\alpha < \alpha_0, \theta < \theta_0$, $A_{\tilde{T},\alpha,\theta}^{iso}(T) > A_{\tilde{T},\alpha,\theta}^{iso}(T_0)$ for any map T that is not locally injective or whose overlapping area is greater than λ .*

Proof. The proof closely follows that of Proposition 5.3 in [2]. In the following, we assume that an arbitrary but fixed set of auxiliary triangles \tilde{T} is used. Also, since T_0 is injective, by Lemma 4.2, there exists some $\theta_0 > 0$ such that $A_{\tilde{T},0,\theta}^{iso}(T_0) = 0$ for all $\theta < \theta_0$. In the following, we consider some fixed θ in this range. For notational convenience, we shall shorthand $A_{\tilde{T},\alpha,\theta}^{iso}$ as A_α^{iso} (not to be confused with IsoTLC).

Since arc-occupancy does not depend on α , IsoSEA shares the same partial derivative as IsoTLC with respect to α , and previous results regarding the derivative of IsoTLC (e.g., Lemma 3.1 (2)) applies to IsoSEA

too. In particular, since T_0 is injective, the derivative $\partial A_\alpha^{iso}(T_0)/\partial\alpha$ is always bounded. We pick an arbitrary but small positive value τ , and let δ be the maximum value of the derivative for all $\alpha < \tau$.

Now consider a map T that is not locally injective, or that $A_{overlap}(T) > \lambda$. We separately consider the cases that (1) T has some small-area triangle (including degenerate triangles), (2) T has some triangle with large Dirichlet energy, and (3) T has neither.

1. Suppose T has a triangle whose unsigned area is smaller than ϵ , which is found by Lemma 3.2 for δ . This case is already considered in the proof of Proposition 3.3, which shows that there exists some $\beta > 0$ such that for any $\alpha < \min(\beta, \tau)$, $\partial A_\alpha^{iso}(T)/\partial\alpha > \partial A_\alpha^{iso}(T_0)/\partial\alpha$. On the other hand, by Lemma 4.2, $A_0^{iso}(T) \geq 0 = A_0^{iso}(T_0)$. Hence $A_\alpha^{iso}(T) > A_\alpha^{iso}(T_0)$ for any $\alpha < \min(\beta, \tau)$.
2. Suppose all triangles in T have unsigned areas no smaller than ϵ , but at least one triangle has a Dirichlet energy greater than η , which is found by Lemma 4.3 for δ . By the lemma, and similar to the case above, there exists some $\gamma > 0$ such that $A_\alpha^{iso}(T) > A_\alpha^{iso}(T_0)$ for any $\alpha < \min(\gamma, \tau)$.
3. Suppose the triangles of T have neither small unsigned areas nor large Dirichlet energy. We further split this case into three sub-cases:
 - T has some inverted triangle. Since each inverted triangle must have an unsigned area no smaller than ϵ , by Lemmas 4.1 and 4.2, $A_\alpha^{iso}(T) \geq A^{excess}(T) \geq A^{invert}(T) \geq \epsilon$ for any $\alpha \geq 0$. Since $A_0^{iso}(T_0) = 0$ and the partial derivative $\partial A_\alpha^{iso}(T_0)/\partial\alpha$ is bounded, we conclude that there exists some $\kappa_1 > 0$ such that, for all $\alpha < \kappa_1$, $A_\alpha^{iso}(T_0) < \epsilon \leq A_\alpha^{iso}(T)$.
 - T has no inverted (or degenerate) triangle, but some vertex v has an angle sum other than 2π . By Lemma 4.4, $A_{overlap}(T) \geq \sigma = \epsilon h^2 \pi / 4\eta$, where h is the smallest height among all auxiliary triangles, and ϵ, η are constants found in cases (1,2) above. Note that σ , like ϵ and η , is independent of the map T . Following Lemmas 4.1 and 4.2, $A_\alpha^{iso}(T) \geq A^{excess}(T) \geq A_{overlap}(T) \geq \sigma$ for any $\alpha \geq 0$. Similar to the previous sub-case, there exists some $\kappa_2 > 0$ such that, for all $\alpha < \kappa_2$, $A_\alpha^{iso}(T_0) < \sigma \leq A_\alpha^{iso}(T)$.
 - T is locally injective but $A_{overlap}(T) > \lambda$. Similar to the previous sub-case, there exists some $\kappa_3 > 0$ such that, for all $\alpha < \kappa_3$, $A_\alpha^{iso}(T_0) < \lambda < A_\alpha^{iso}(T)$.

The proof is completed by setting $\alpha_0 = \min(\tau, \beta, \gamma, \kappa_1, \kappa_2, \kappa_3)$. \square

5 Implementation details

Minimizing IsoTLC and IsoSEA using gradient-based solvers requires the evaluation of the energies, their gradients (for quasi-Newton), and Hessians (for projected Newton). We provide more implementation details in this section.

5.1 IsoTLC

Evaluating IsoTLC amounts to summing up the per-element *isometric lifted content*, defined in Equation 6 in the paper, which in turn can be directly obtained from the area (or volume) of the d -dimensional element t , the auxiliary element \tilde{t} , and the lifted element. In particular, as derived in [1] (Section 4.2.1), the area (or volume) of the lifted element at scale α has the form:

$$A_{\tilde{t}, \alpha}(t) = \frac{1}{d!} \sqrt{\text{Det}(X^T X + \alpha \tilde{X}^T \tilde{X})}$$

where X (respectively \tilde{X}) is the $d \times d$ matrix whose column vectors are the edge vectors from one vertex of the simplex t (respectively \tilde{t}) to the other d vertices of the simplex.

To derive the gradient and Hessian of IsoTLC, we resort to the general technique proposed by Smith et al. [8] for distortion energies in both 2D or 3D. We shall give details on the application of this technique to IsoTLC, and we refer the reader to the paper [8] and a comprehensive course note [4] for in-depth discussions of the general technique.

Smith's technique assumes distortion energies of the general form

$$\Psi(T) = \sum_{t \in T} A_t \Psi_t(L)$$

Here, $A_t \Psi_t(L)$ is the per-simplex distortion $\Psi_t(L)$ weighted by the area (or volume) of the rest (auxiliary) simplex t . The distortion is defined using L , which is the linear transformation that maps the edge vectors \tilde{X} of t to the edge vectors X of t . L is often called the *deformation gradient*. Smith's technique applies to any distortion Ψ_t that can be written in terms of three invariants:

$$I_1 = \sum_i \sigma_i, \quad I_2 = \sum_i \sigma_i^2, \quad I_3 = \prod_i \sigma_i \quad (14)$$

where σ_i are the singular values of L .

The per-simplex term in IsoTLC is the isometric lifted content, $A_{t,\alpha}^{iso}(t)$. From its singular-value form (Equation 7 in the paper), we obtain

$$A_{t,\alpha}^{iso}(t) = A_t \Psi_{t,\alpha}(L), \quad (15)$$

where

$$\Psi_{t,\alpha}(L) = \sqrt{\Pi_{i=1}^d \sigma_i^2 + \frac{\alpha}{2^{d-1}} \Pi_{i=1}^d (\sigma_i^2 + 1) + \alpha^2}. \quad (16)$$

We can rewrite Equation 16 in terms of the invariants in Equations 14 for a triangle ($d = 2$),

$$\Psi_{t,\alpha}(L) = \sqrt{(1 + \frac{\alpha}{2}) I_3^2 + \frac{\alpha}{2} I_2 + \frac{\alpha}{2} + \alpha^2}, \quad (17)$$

and for a tetrahedron ($d = 3$),

$$\Psi_{t,\alpha}(L) = \sqrt{(1 + \frac{\alpha}{4}) I_3^2 + \frac{\alpha}{4} I_2 + \frac{\alpha}{8} (I_2^2 - II_C) + \frac{\alpha}{4} + \alpha^2}, \quad (18)$$

where $II_C = \|L^T L\|^2$ can also be expressed in terms of the invariants (see Appendix A of [8]),

$$II_C = \frac{1}{2} I_2^2 - \frac{1}{2} I_1^4 + I_1^2 I_2 + 4 I_1 I_3.$$

To evaluate the gradient of the isometric lifted content, $A_{t,\alpha}^{iso}(t)$, we flatten t 's vertex coordinates into a vector \mathbf{x} and apply the chain rule,

$$\frac{\partial A_{t,\alpha}^{iso}}{\partial \mathbf{x}} = A_t \frac{\partial \Psi_{t,\alpha}}{\partial L} \frac{\partial L}{\partial \mathbf{x}} = A_t \left(\sum_{i=1}^3 \frac{\partial \Psi_{t,\alpha}}{\partial I_i} \frac{\partial I_i}{\partial L} \right) \frac{\partial L}{\partial \mathbf{x}}. \quad (19)$$

Since $\Psi_{t,\alpha}$ is a scalar function of the three invariants, the explicit formula for its partial derivatives $\frac{\partial \Psi_{t,\alpha}}{\partial I_i}$ can be obtained using calculus. The formulas for $\frac{\partial I_i}{\partial L}$ are provided in [8] and Appendix B of [4]. Finally, Appendix E of [4] describes how to compute $\frac{\partial L}{\partial \mathbf{x}}$.

Optimizing IsoTLC using projected Newton requires a positive semi-definite (PSD) projection of the Hessian. One approach is first evaluating the Hessian matrix of the isometric lifted content $A_{t,\alpha}^{iso}(t)$ for each simplex, then numerically projecting it to be positive semi-definite, and finally assembling the full Hessian by accumulating per-simplex Hessians. Smith et al. [8] introduced a general routine to obtain per-simplex PSD-projected Hessian without first evaluating the original Hessian matrix, provided that the distortion energy can be written in terms of the three invariants. The routine is described in details in [8] and chapter 7 of [4]. In practice, we found that using the projected Hessian of the residual $R^{iso}(t)$ instead of $A_{t,\alpha}^{iso}(t)$ leads to a higher success rate and lower distortions on the benchmark. Recall that $R^{iso}(t)$ is the difference between the isometric lifted content $A_{t,\alpha}^{iso}(t)$ and the signed volume $A(t)$ (Equation 8 in the paper). The residual can also be written in terms of the three invariants in 2D,

$$R^{iso}(t) = A_t \left(\sqrt{(1 + \frac{\alpha}{2}) I_3^2 + \frac{\alpha}{2} I_2 + \frac{\alpha}{2} + \alpha^2} - I_3 \right), \quad (20)$$

and in 3D,

$$R^{iso}(t) = A_{\tilde{t}} \left(\sqrt{(1 + \frac{\alpha}{4})I_3^2 + \frac{\alpha}{4}I_2 + \frac{\alpha}{8}(I_2^2 - II_C)} + \frac{\alpha}{4} + \alpha^2 - I_3 \right). \quad (21)$$

We provide the pseudo-code to evaluate projected Hessians of the residual $R^{iso}(t)$ in 2D (Algorithm 1) and 3D (Algorithm 2) using the technique in [8].

Algorithm 1 Evaluate projected Hessian of the residual $R^{iso}(t)$ in 2D

Require: α , coordinates $\tilde{\mathbf{x}}$ of \tilde{t} , coordinates \mathbf{x} of t

- ```

1: $L \leftarrow \text{deformationGradient}(\tilde{\mathbf{x}}, \mathbf{x})$ ▷ See Appendix D of [4] for computing L
2: $U, \Sigma, V \leftarrow \text{SVD}(L)$ ▷ Rotation-variant SVD, see Appendix F of [4]
3: $\sigma_1, \sigma_2 \leftarrow \text{diagonal}(\Sigma)$
4: $I_1 \leftarrow \sigma_1 + \sigma_2$
5: $I_2 \leftarrow \sigma_1^2 + \sigma_2^2$
6: $I_3 \leftarrow \sigma_1 \sigma_2$
7: $\psi \leftarrow \sqrt{(1 + \frac{\alpha}{2})I_3^2 + \frac{\alpha}{2}I_2 + \frac{\alpha}{2} + \alpha^2}$ ▷ $A_{\tilde{t}}\psi$ is the isometric lifted content
8: $\lambda_{twist} \leftarrow (\frac{\alpha}{2} + (1 + \frac{\alpha}{2})I_3)/\psi - 1$
9: $v_{twist} \leftarrow \text{vec}(\frac{1}{\sqrt{2}}U \begin{bmatrix} 0 & -1 \\ 1 & 0 \end{bmatrix} V^\top)$ ▷ $\text{vec}(\cdot)$ flattens a matrix into a vector. See section 3 of [8]
10: $\lambda_{flip} \leftarrow (\frac{\alpha}{2} - (1 + \frac{\alpha}{2})I_3)/\psi + 1$
11: $v_{flip} \leftarrow \text{vec}(\frac{1}{\sqrt{2}}U \begin{bmatrix} 0 & 1 \\ 1 & 0 \end{bmatrix} V^\top)$
12: $d_1 \leftarrow \text{vec}(U \begin{bmatrix} 1 & 0 \\ 0 & 0 \end{bmatrix} V^\top)$
13: $d_2 \leftarrow \text{vec}(U \begin{bmatrix} 0 & 0 \\ 0 & 1 \end{bmatrix} V^\top)$
14: $a_{11} \leftarrow (\frac{\alpha}{2} + \alpha^2 + \frac{\alpha}{2}\sigma_2^2)(\frac{\alpha}{2} + (1 + \frac{\alpha}{2})\sigma_2^2)/\psi^3$
15: $a_{22} \leftarrow (\frac{\alpha}{2} + \alpha^2 + \frac{\alpha}{2}\sigma_1^2)(\frac{\alpha}{2} + (1 + \frac{\alpha}{2})\sigma_1^2)/\psi^3$
16: $a_{12} \leftarrow (\alpha + \frac{9}{4}\alpha^2 + \alpha^3 + (1 + \frac{\alpha}{2})(\frac{\alpha}{2}I_2 + (1 + \frac{\alpha}{2})I_3^2))I_3/\psi^3 - 1$
17: if $a_{12} = 0$ then
18: $\lambda_{scale_1} \leftarrow a_{11}$
19: $\lambda_{scale_2} \leftarrow a_{22}$
20: $v_{scale_1} \leftarrow d_1$
21: $v_{scale_2} \leftarrow d_2$
22: else
23: $A \leftarrow \begin{bmatrix} a_{11} & a_{12} \\ a_{12} & a_{22} \end{bmatrix}$
24: $\lambda_{scale_1}, \lambda_{scale_2} \leftarrow \text{eigenValues}(A)$
25: $\beta \leftarrow (\lambda_{scale_1} - a_{22})/a_{12}$
26: $v_{scale_1} \leftarrow (\beta d_1 + d_2)/\sqrt{1 + \beta^2}$
27: $v_{scale_2} \leftarrow (d_1 - \beta d_2)/\sqrt{1 + \beta^2}$
28: end if
29: $H_L \leftarrow \sum_{i \in \{twist, flip, scale_1, scale_2\}} \max(\lambda_i, 0)v_i v_i^\top$
30: $H_{\mathbf{x}} \leftarrow \text{area}(\tilde{\mathbf{x}})(\frac{\partial L}{\partial \mathbf{x}})^\top H_L \frac{\partial L}{\partial \mathbf{x}}$ ▷ See Appendix E of [4] for computing $\frac{\partial L}{\partial \mathbf{x}}$
31: return $H_{\mathbf{x}}$

```
- 

## 5.2 IsoSEA

The IsoSEA energy is the difference between the IsoTLC energy and the *arc-occupancy* of the boundary of the mapped domain. This latter term was proposed in [2], which gave a detailed account of its derivation (Section 5.2) and computation (Section 6). Here we give an abbreviated account of arc-occupancy, and we refer readers to [2] for a full discussion.

---

**Algorithm 2** Evaluate projected Hessian of the residual  $R^{iso}(t)$  in 3D

---

**Require:**  $\alpha$ , coordinates  $\tilde{\mathbf{x}}$  of  $\tilde{t}$ , coordinates  $\mathbf{x}$  of  $t$

1:  $L \leftarrow \text{deformationGradient}(\tilde{\mathbf{x}}, \mathbf{x})$  ▷ See Appendix D of [4] for computing  $L$   
 2:  $U, \Sigma, V \leftarrow \text{SVD}(L)$  ▷ Rotation-variant SVD, see Appendix F of [4]  
 3:  $\sigma_1, \sigma_2, \sigma_3 \leftarrow \text{diagonal}(\Sigma)$   
 4:  $I_1 \leftarrow \sigma_1 + \sigma_2 + \sigma_3$   
 5:  $I_2 \leftarrow \sigma_1^2 + \sigma_2^2 + \sigma_3^2$   
 6:  $I_3 \leftarrow \sigma_1 \sigma_2 \sigma_3$   
 7:  $II_C \leftarrow \sigma_1^4 + \sigma_2^4 + \sigma_3^4$   
 8:  $II_C^* \leftarrow \sigma_1^2 \sigma_2^2 + \sigma_1^2 \sigma_3^2 + \sigma_2^2 \sigma_3^2$   
 9:  $\psi \leftarrow \sqrt{(1 + \frac{\alpha}{4})I_3^2 + \frac{\alpha}{4}I_2 + \frac{\alpha}{8}(I_2^2 - II_C) + \frac{\alpha}{4} + \alpha^2}$  ▷  $A_{\tilde{t}}\psi$  is the isometric lifted content  
 10:  $c_1 \leftarrow 1 + \frac{\alpha}{4}$   
 11:  $c_2 \leftarrow \frac{\alpha}{4}$   
 12:  $c_3 \leftarrow \frac{\alpha}{8}$   
 13:  $c_4 \leftarrow \frac{\alpha}{4} + \alpha^2$   
 14:  $\lambda_{twist_1} \leftarrow (c_2 + 2c_3(\sigma_1^2 + \sigma_2 \sigma_3) + c_1 \sigma_1 I_3)/\psi - \sigma_1$   
 15:  $v_{twist_1} \leftarrow \text{vec}(\frac{1}{\sqrt{2}}U \begin{bmatrix} 0 & 0 & 0 \\ 0 & 0 & 1 \\ 0 & -1 & 0 \end{bmatrix} V^\top)$  ▷  $\text{vec}(\cdot)$  flattens a matrix into a vector. See section 3 of [8]  
 16:  $\lambda_{twist_2} \leftarrow (c_2 + 2c_3(\sigma_2^2 + \sigma_1 \sigma_3) + c_1 \sigma_2 I_3)/\psi - \sigma_2$   
 17:  $v_{twist_2} \leftarrow \text{vec}(\frac{1}{\sqrt{2}}U \begin{bmatrix} 0 & 0 & 1 \\ 0 & 0 & 0 \\ -1 & 0 & 0 \end{bmatrix} V^\top)$   
 18:  $\lambda_{twist_3} \leftarrow (c_2 + 2c_3(\sigma_3^2 + \sigma_1 \sigma_2) + c_1 \sigma_3 I_3)/\psi - \sigma_3$   
 19:  $v_{twist_3} \leftarrow \text{vec}(\frac{1}{\sqrt{2}}U \begin{bmatrix} 0 & -1 & 0 \\ 1 & 0 & 0 \\ 0 & 0 & 0 \end{bmatrix} V^\top)$   
 20:  $\lambda_{flip_1} \leftarrow (c_2 + 2c_3(\sigma_1^2 - \sigma_2 \sigma_3) - c_1 \sigma_1 I_3)/\psi + \sigma_1$   
 21:  $v_{flip_1} \leftarrow \text{vec}(\frac{1}{\sqrt{2}}U \begin{bmatrix} 0 & 0 & 0 \\ 0 & 0 & 1 \\ 0 & 1 & 0 \end{bmatrix} V^\top)$   
 22:  $\lambda_{flip_2} \leftarrow (c_2 + 2c_3(\sigma_2^2 - \sigma_1 \sigma_3) - c_1 \sigma_2 I_3)/\psi + \sigma_2$   
 23:  $v_{flip_2} \leftarrow \text{vec}(\frac{1}{\sqrt{2}}U \begin{bmatrix} 0 & 0 & 1 \\ 0 & 0 & 0 \\ 1 & 0 & 0 \end{bmatrix} V^\top)$   
 24:  $\lambda_{flip_3} \leftarrow (c_2 + 2c_3(\sigma_3^2 - \sigma_1 \sigma_2) - c_1 \sigma_3 I_3)/\psi + \sigma_3$   
 25:  $v_{flip_3} \leftarrow \text{vec}(\frac{1}{\sqrt{2}}U \begin{bmatrix} 0 & 1 & 0 \\ 1 & 0 & 0 \\ 0 & 0 & 0 \end{bmatrix} V^\top)$   
 26:  $d_1 \leftarrow \text{vec}(U \begin{bmatrix} 1 & 0 & 0 \\ 0 & 0 & 0 \\ 0 & 0 & 0 \end{bmatrix} V^\top)$   
 27:  $d_2 \leftarrow \text{vec}(U \begin{bmatrix} 0 & 0 & 0 \\ 0 & 1 & 0 \\ 0 & 0 & 0 \end{bmatrix} V^\top)$   
 28:  $d_3 \leftarrow \text{vec}(U \begin{bmatrix} 0 & 0 & 0 \\ 0 & 0 & 0 \\ 0 & 0 & 1 \end{bmatrix} V^\top)$   
 29:  $a_{11} \leftarrow (c_4 + 2c_3 \sigma_2^2 \sigma_3^2 + c_2(\sigma_2^2 + \sigma_3^2))(c_2 + c_1 \sigma_2^2 \sigma_3^2 + 2c_3(\sigma_2^2 + \sigma_3^2))/\psi^3$   
 30:  $a_{22} \leftarrow (c_4 + 2c_3 \sigma_1^2 \sigma_3^2 + c_2(\sigma_1^2 + \sigma_3^2))(c_2 + c_1 \sigma_1^2 \sigma_3^2 + 2c_3(\sigma_1^2 + \sigma_3^2))/\psi^3$   
 31:  $a_{33} \leftarrow (c_4 + 2c_3 \sigma_1^2 \sigma_2^2 + c_2(\sigma_1^2 + \sigma_2^2))(c_2 + c_1 \sigma_1^2 \sigma_2^2 + 2c_3(\sigma_1^2 + \sigma_2^2))/\psi^3$

---

---

32:  $a_{12} \leftarrow (c_2(c_1 I_3 \sigma_3(I_2 + \sigma_3^2) + 2c_3 \sigma_1 \sigma_2(I_2 - \sigma_3^2) - \psi I_2 \sigma_3) + 4c_3^2 \sigma_1 \sigma_2(II_C^* - \sigma_3^4) + 2c_3(2c_4 \sigma_1 \sigma_2 - \psi II_C^* \sigma_3 + c_1 I_3(II_C^* + \sigma_1^2 \sigma_2^2) \sigma_3) + (c_1 I_3^2(c_1 I_3 - \psi) - c_4(\psi - 2c_1 I_3))\sigma_3 - c_2^2 \sigma_1^2 \sigma_2^2)/\psi^3$   
 33:  $a_{13} \leftarrow (c_2(c_1 I_3 \sigma_2(I_2 + \sigma_2^2) + 2c_3 \sigma_1 \sigma_3(I_2 - \sigma_2^2) - \psi I_2 \sigma_2) + 4c_3^2 \sigma_1 \sigma_3(II_C^* - \sigma_2^4) + 2c_3(2c_4 \sigma_1 \sigma_3 - \psi II_C^* \sigma_2 + c_1 I_3(II_C^* + \sigma_1^2 \sigma_3^2) \sigma_2) + (c_1 I_3^2(c_1 I_3 - \psi) - c_4(\psi - 2c_1 I_3))\sigma_2 - c_2^2 \sigma_1^2 \sigma_3^2)/\psi^3$   
 34:  $a_{23} \leftarrow (c_2(c_1 I_3 \sigma_1(I_2 + \sigma_1^2) + 2c_3 \sigma_2 \sigma_3(I_2 - \sigma_1^2) - \psi I_2 \sigma_1) + 4c_3^2 \sigma_2 \sigma_3(II_C^* - \sigma_1^4) + 2c_3(2c_4 \sigma_2 \sigma_3 - \psi II_C^* \sigma_1 + c_1 I_3(II_C^* + \sigma_2^2 \sigma_3^2) \sigma_1) + (c_1 I_3^2(c_1 I_3 - \psi) - c_4(\psi - 2c_1 I_3))\sigma_1 - c_2^2 \sigma_2^2 \sigma_3^2)/\psi^3$   
 35: **if**  $a_{12} = 0$  and  $a_{13} = 0$  and  $a_{23} = 0$  **then**  
 36:    $\lambda_{scale_1} \leftarrow a_{11}$   
 37:    $\lambda_{scale_2} \leftarrow a_{22}$   
 38:    $\lambda_{scale_3} \leftarrow a_{33}$   
 39:    $v_{scale_1} \leftarrow d_1$   
 40:    $v_{scale_2} \leftarrow d_2$   
 41:    $v_{scale_3} \leftarrow d_3$   
 42: **else**  
 43:    $A \leftarrow \begin{bmatrix} a_{11} & a_{12} & a_{13} \\ a_{12} & a_{22} & a_{23} \\ a_{13} & a_{23} & a_{33} \end{bmatrix}$   
 44:    $\lambda_{scale_1}, \lambda_{scale_2}, \lambda_{scale_3} \leftarrow \text{eigenValues}(A)$   
 45:    $z_1, z_2, z_3 \leftarrow \text{eigenVectors}(A)$  ▷ normalized eigen vectors, i.e.,  $\|z_i\| = 1$   
 46:    $D \leftarrow [d_1 \quad d_2 \quad d_3]$  ▷ matrix  $D$  with column vectors  $d_1, d_2, d_3$   
 47:    $v_{scale_1} \leftarrow Dz_1$   
 48:    $v_{scale_2} \leftarrow Dz_2$   
 49:    $v_{scale_3} \leftarrow Dz_3$   
 50: **end if**  
 51:  $H_L \leftarrow \sum_{i \in \{twist_1, twist_2, twist_3, flip_1, flip_2, flip_3, scale_1, scale_2, scale_3\}} \max(\lambda_i, 0) v_i v_i^\top$   
 52:  $H_x \leftarrow \text{volume}(\tilde{x})(\frac{\partial L}{\partial x})^\top H_L \frac{\partial L}{\partial x}$  ▷ See Appendix E of [4] for computing  $\frac{\partial L}{\partial x}$   
 53: **return**  $H_x$

---

Consider a triangular mesh  $T$  in the plane with an oriented boundary  $\partial T$  (which may consist of one or multiple curves). To compute arc-occupancy, we construct, for each edge  $e \in \partial T$ , a circular arc with center angle  $\theta$  and  $e$  as its chord. This arc,  $\Gamma_\theta(e)$ , has the same orientation as  $e$  and lies on the right side of  $e$ . We call  $\Gamma_\theta(e)$  the *arc-edge* of  $e$ , and the curve consisting of all arc-edges the *arc-boundary* of  $\partial T$ , denoted by  $\Gamma_\theta(\partial T)$ . Additionally, we call the area bounded by each edge  $e$  and its arc-edge a “flap” (see Figure 5 left of [2]). The arc-occupancy of  $\partial T$  is defined as the occupancy of the arc-boundary minus the sum of all the flap areas, denoted as  $B_\theta(\partial T)$ :

$$O_\theta(\partial T) = O(\Gamma_\theta(\partial T)) - B_\theta(\partial T) \quad (22)$$

The second term of Equation 22,  $B_\theta(\partial T)$ , has a simple expression:

$$B_\theta(\partial T) = \sum_{e \in \partial T} \frac{\|e\|^2(\theta - \sin \theta)}{4(1 - \cos \theta)}.$$

Evaluating the first term of Equation 22, the occupancy of the arc-boundary  $\Gamma_\theta(\partial T)$ , amounts to computing the arrangement of the arc-boundary and the winding number of each region in the arrangement. The occupancy is the sum of area of all regions with a positive winding number. Please refer to [2] (Section 6) for details of computing such arrangement, the winding numbers, and the region areas. Finally, since both terms of Equation 22 can be expressed as functions of the locations of the vertices of  $\partial T$ , the gradient of  $O_\theta(\partial T)$  can be derived using the chain rule.

## 6 Additional results

### 6.1 Benchmark examples

We show more comparisons between our method and competing methods, including TLC [1], SEA [2], and FFM [3], using examples from the fixed-boundary [1] and free-boundary [2] benchmarks.

Figure 1 shows several 2D examples from the fixed-boundary benchmark. The initial maps in these examples contain tens to hundreds inverted triangles. While TLC, FFM and our IsoTLC method successfully recover injectivity in all examples, IsoTLC achieves the lowest isometric distortion among the three methods.

Figure 2 shows several examples from the free-boundary benchmark. Each example contains up to 20 constrained vertices, and the initial map has inverted triangles, overwound vertices, and large areas of overlap between triangles. While both SEA and our IsoSEA method successfully recover injectivity in all examples, IsoSEA achieves significantly lower isometric distortions.

### 6.2 Failure cases of IsoTLC

Even though our IsoTLC method successfully produced injective maps for all examples in the fixed-boundary benchmark of [1], there is no guarantee that it (or the original TLC method) will always succeed. Here we investigate several reasons that may cause IsoTLC to fail to produce injective maps.

The first reason is that the mapping problem does not have an injective solution for the given mesh structure and boundary (and possibly other positional) constraints. Figure 3 shows two such examples taken from [9], where an injective solution is known to not exist for the respective target boundary (if the mesh structure is not allowed to change). Our method cannot produce injective maps for either problem, and the resulting maps still contain flipped triangles.

The second reason is that the energy converges slowly or the solver gets stuck at a non-injective local minimum. Slow or stalled convergence often arises when the initial map is too far from an injective map. We show several such failure examples in Figures 4 and 5, both taken from [3] (except for the bottom one in Figure 4). In Figure 4, the “Lucy” mesh is mapped to the outline of letter “P” but initialized with two different randomized maps (instead of Tutte embedding as done in our main experiment on the benchmark). Optimizing TLC (using either QN or PN) fails to produce an injective map within the maximum number of iterations (10,000) starting from either initial state. Optimizing IsoTLC produces an injective map starting from one of the initial maps but fails on the other. In Figure 5, we took a tetrahedral mesh sandwiched between an outer cube and an inner cube and rotated those vertices on the inner cube by various degrees. Our IsoTLC method produces an injective map for rotations by 45°, 90° and 180° but fails for 135° (TLC

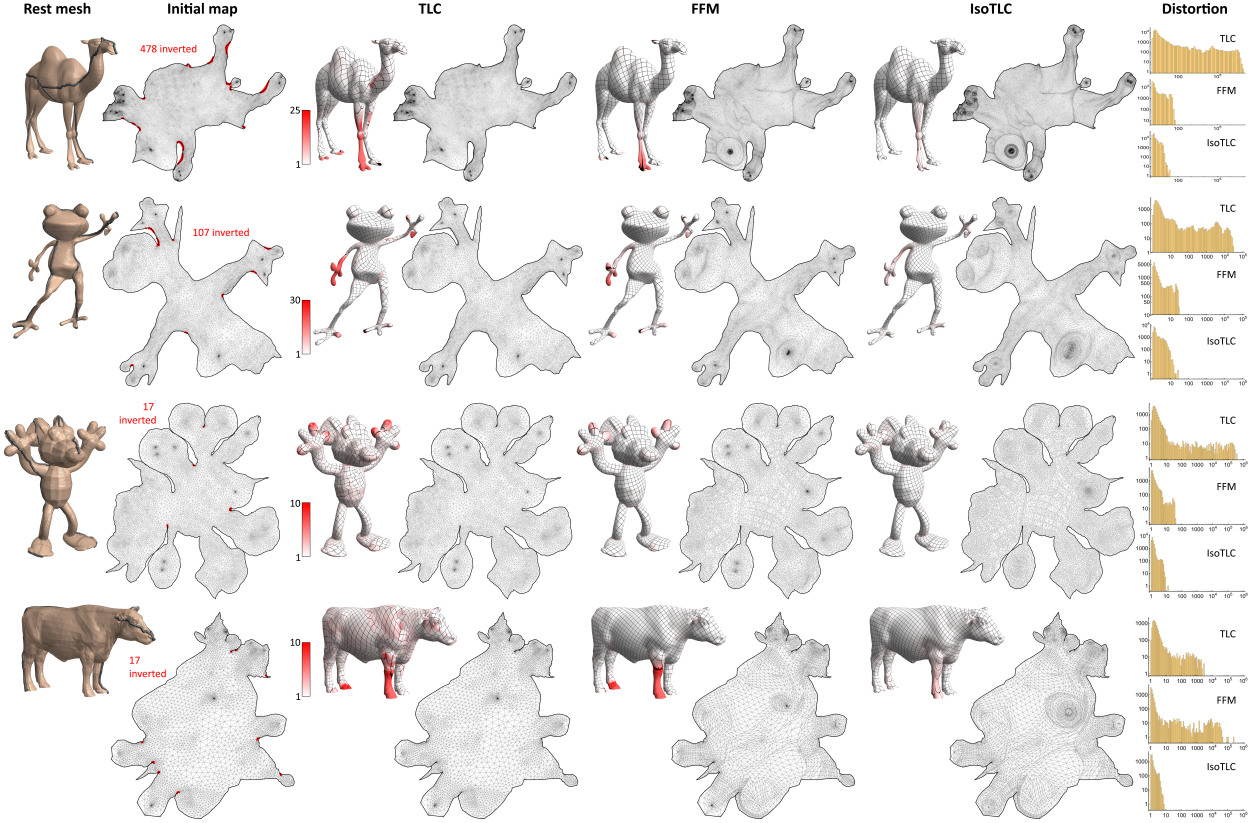


Figure 1: Comparing maps computed by TLC [1], FFM [3], and our method (IsoTLC) on several 2D examples in the fixed-boundary benchmark of [1]. Each example consists of a rest mesh and an initial map containing inverted triangles (red). Histograms of per-element distortion are shown using the distortion measure  $\max(\sigma_1, 1/\sigma_2)$ .

succeeds only on  $45^\circ$  and  $90^\circ$ ). The FFM method of [3] succeeds in producing injective maps for almost all examples in these two figures, except for the second random initialization of Figure 4.

### 6.3 Handling poor triangulations

Finally, we demonstrate our IsoTLC method on meshes containing poorly shaped elements in Figure 6. These meshes were taken from Thingi10K [10] (id: 662115), and the triangulations are highly anisotropic. To make sure that the problem is feasible, for each mesh  $M$ , we first employed the algorithm of [5] to find a cut as well as a globally injective map  $T$  to the plane. To test IsoTLC, we fixed the boundary  $\partial T$  and created the initial non-injective map by re-embedding  $M$  into  $\partial T$  using Tutte. We observed that both TLC and IsoTLC succeeded in producing injective maps for all tested examples, while IsoTLC achieved much lower distortion.

## References

- [1] Xingyi Du, Noam Aigerman, Qingnan Zhou, Shahar Z Kovalsky, Yajie Yan, Danny M Kaufman, and Tao Ju. Lifting simplices to find injectivity. *ACM Transactions on Graphics (TOG)*, 39(4):120–1, 2020.
- [2] Xingyi Du, Danny M Kaufman, Qingnan Zhou, Shahar Z Kovalsky, Yajie Yan, Noam Aigerman, and Tao Ju. Optimizing global injectivity for constrained parameterization. *ACM Transactions on Graphics (TOG)*, 40(6):1–18, 2021.

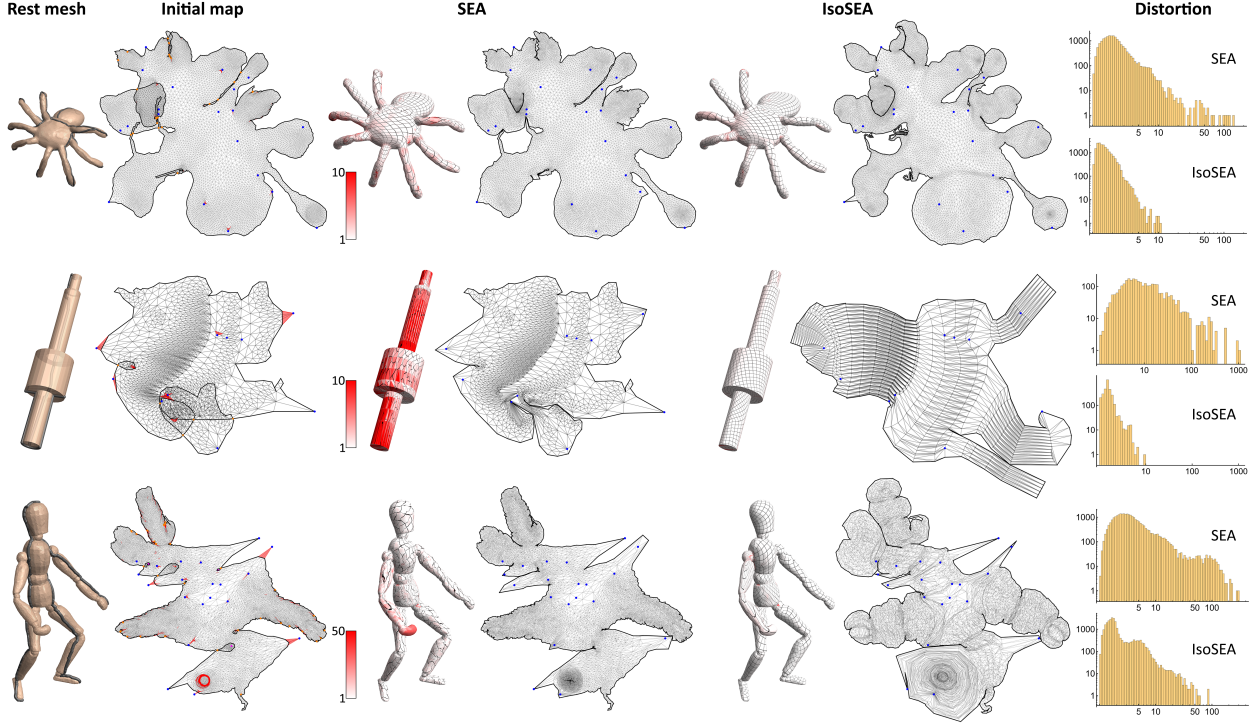


Figure 2: Comparing maps computed by SEA [2] and our method (IsoSEA) on several examples in the free-boundary benchmark of [2]. Each example consists of a rest mesh, a set of constrained vertices (blue), and an initial map containing inverted triangles (red), overwound vertices (purple), and global overlaps. Histograms of per-element distortion are shown using the distortion measure  $\max(\sigma_1, 1/\sigma_2)$ .

- [3] Vladimir Garanzha, Igor Kaporin, Liudmila Kudryavtseva, François Protais, Nicolas Ray, and Dmitry Sokolov. Foldover-free maps in 50 lines of code. *ACM Transactions on Graphics (TOG)*, 40(4):1–16, 2021.
- [4] Theodore Kim and David Eberle. Dynamic deformables: implementation and production practicalities (now with code!). *ACM SIGGRAPH 2022 Courses*, 2022.
- [5] Minchen Li, Danny M. Kaufman, Vladimir G. Kim, Justin Solomon, and Alla Sheffer. Optcuts: Joint optimization of surface cuts and parameterization. *ACM Transactions on Graphics*, 37(6), 2018.
- [6] Yaron Lipman. Bijective mappings of meshes with boundary and the degree in mesh processing. *SIAM Journal on Imaging Sciences [electronic only]*, 7, 04 2014.
- [7] Ulrich Pinkall and Konrad Polthier. Computing discrete minimal surfaces and their conjugates. *Experimental mathematics*, 2(1):15–36, 1993.
- [8] Breannan Smith, Fernando De Goes, and Theodore Kim. Analytic eigensystems for isotropic distortion energies. *ACM Transactions on Graphics (TOG)*, 38(1):1–15, 2019.
- [9] Ofir Weber and Denis Zorin. Locally injective parametrization with arbitrary fixed boundaries. *ACM Transactions on Graphics (TOG)*, 33(4):75, 2014.
- [10] Qingnan Zhou and Alec Jacobson. Thingi10k: A dataset of 10,000 3d-printing models. *arXiv preprint arXiv:1605.04797*, 2016.

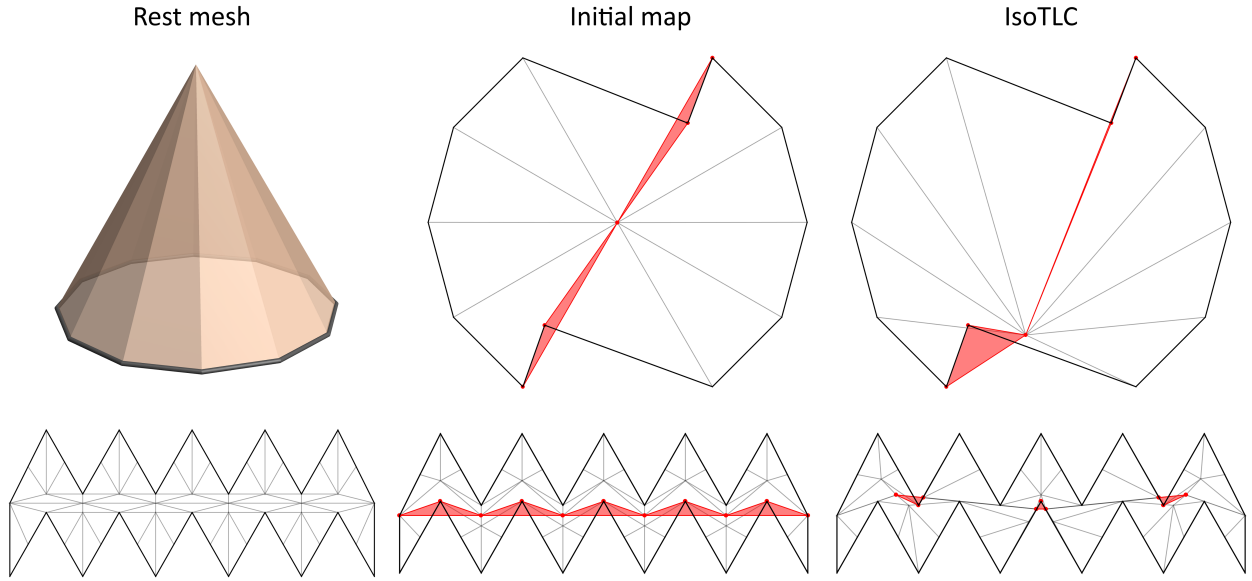


Figure 3: Two fixed-boundary mapping examples (top and bottom) taken from [9] where an injective map does not exist for the given target boundary (without changing the mesh structure). Our IsoTLC method cannot produce injective maps for such problems.

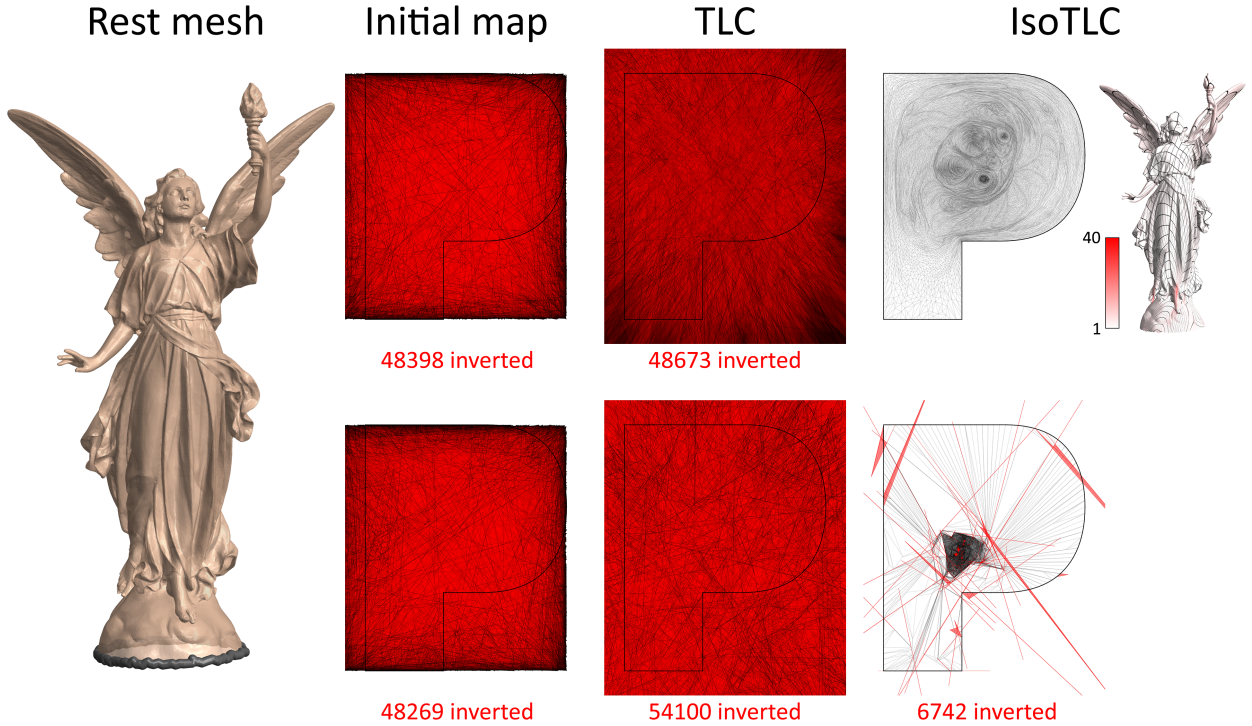


Figure 4: Two fixed-boundary examples (top and bottom), mapping the “Lucy” mesh to the outline of letter “P”, initialized with two random maps. The top example is taken from [3]. IsoTLC succeeds in the top example but fails to produce an injective map within 10000 iterations (using either QN or PN) on the bottom one. TLC fails on both examples.

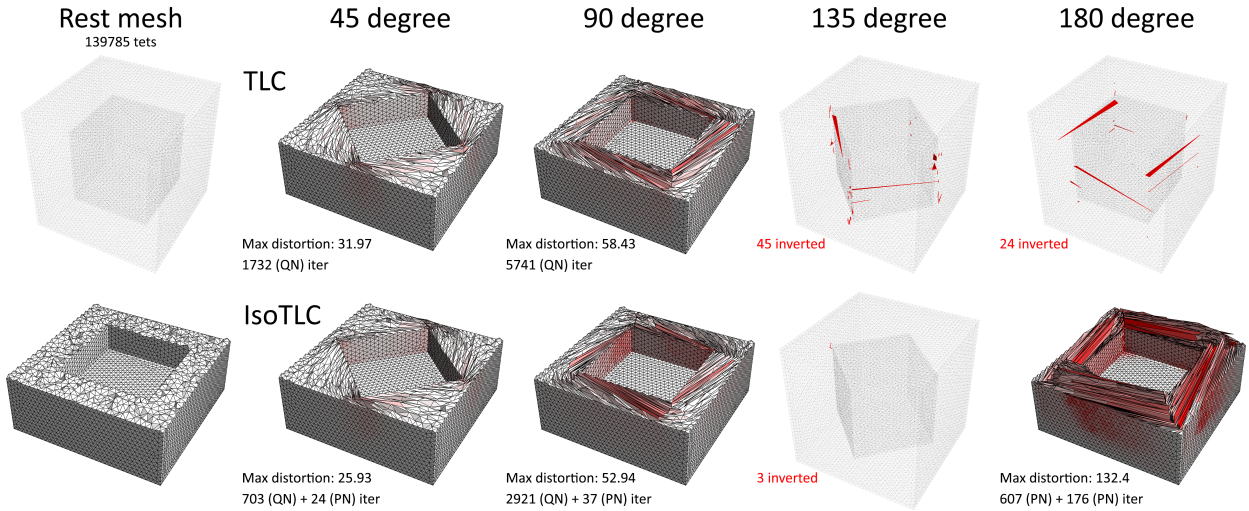


Figure 5: Mapping a tetrahedral mesh bounded by two cubical surfaces after rotating the inner cube by various degrees (clockwise as viewed from the top). IsoTLC produces injective maps for rotations by  $45^\circ$ ,  $90^\circ$  and  $180^\circ$  but fails for  $135^\circ$ . TLC succeeds only on  $45^\circ$  and  $90^\circ$ . We note the number of solver iterations (and solver type) for each method (iterations for the two phases of optimizing IsoTLC are shown separately).

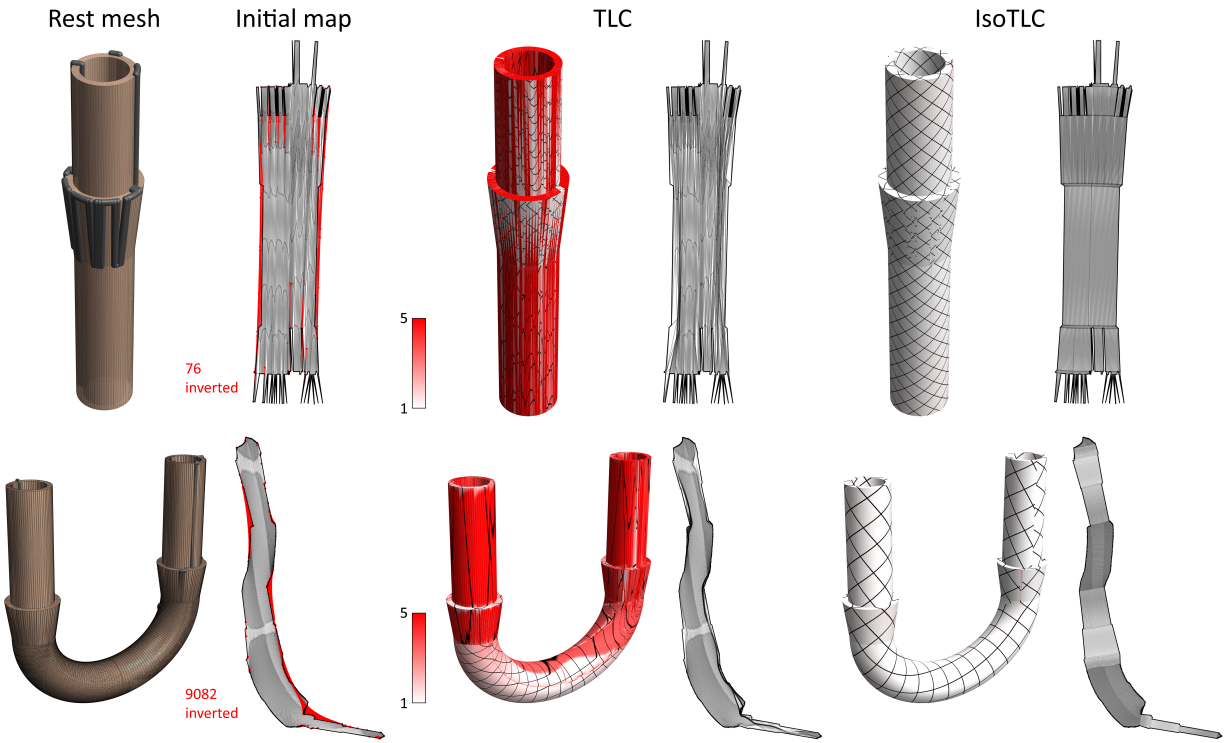


Figure 6: Fixed-boundary mapping of meshes with poorly shaped triangles from Thingi10K. Both TLC and IsoTLC succeeded in producing injective maps, while IsoTLC achieved much lower distortion.